THE JOURNAL OF BIOLOGICAL CHEMISTRY VOL. 290, NO. 15, pp. 9896–9905, April 10, 2015

Myeloperoxidase-dependent Lipid Peroxidation Promotes the Oxidative Modification of Cytosolic Proteins in Phagocytic Neutrophils*

Received for publication, September 21, 2014, and in revised form, February 10, 2015 Published, JBC Papers in Press, February 19, 2015, DOI 10.1074/jbc.M114.613422

Rachel P. Wilkie-Grantham[1], Nicholas J. Magon[1], D. Tim Harwood, Anthony J. Kettle, Margreet C. Vissers, Christine C. Winterbourn, and Mark B. Hampton[2]

From the Centre for Free Radical Research, Department of Pathology, University of Otago, Christchurch 8140, New Zealand

Background: Neutrophils generate oxidants to kill microbes ingested into phagosomes, but extraphagosomal protein oxidation may also occur.
Results: Specific neutrophil cytosolic proteins were carbonylated following phagocytosis; carbonylation was impaired by myeloperoxidase inhibitors or radical scavengers that inhibit lipid peroxidation.
Conclusion: Lipid peroxidation in the phagosomal membrane leads to oxidation of cytosolic proteins.
Significance: Protein oxidation may influence the function and fate of post-phagocytic neutrophils.

Phagocytic neutrophils generate reactive oxygen species to kill microbes. Oxidant generation occurs within an intracellular phagosome, but diffusible species can react with the neutrophil and surrounding tissue. To investigate the extent of oxidative modification, we assessed the carbonylation of cytosolic proteins in phagocytic neutrophils. A 4-fold increase in protein carbonylation was measured within 15 min of initiating phagocytosis. Carbonylation was dependent on NADPH oxidase and myeloperoxidase activity and was inhibited by butylated hydroxytoluene and Trolox, indicating a role for myeloperoxidase-dependent lipid peroxidation. Proteomic analysis of target proteins revealed significant carbonylation of the S100A9 subunit of calprotectin, a truncated form of Hsp70, actin, and hemoglobin from contaminating erythrocytes. The addition of the reactive aldehyde 4-hydroxynonenal (HNE) caused carbonylation, and HNE-glutathione adducts were detected in the cytosol of phagocytic neutrophils. The post-translational modification of neutrophil proteins will influence the functioning and fate of these immune cells in the period following phagocytic activation, and provides a marker of neutrophil activation during infection and inflammation.

Neutrophils play a crucial role in inflammation through the phagocytosis and destruction of invading pathogens. Phagocytosis stimulates the assembly of the NOX2 NADPH oxidase complex in the phagosomal membrane, which reduces oxygen to superoxide (1). The superoxide dismutates to hydrogen peroxide, which is a substrate for myeloperoxidase in the generation of microbicidal hypohalous acids (2). The localization of oxidant generation to the phagosome helps limit potential damage to surrounding tissues, but adventitious release of myeloperoxidase and the diffusion of reactive species enable extraphagosomal oxidation.

There have been relatively few investigations of extraphagosomal protein modification in activated neutrophils. It is known that chlorotyrosine generated by hypochlorous acid during phagocytosis is mostly on neutrophil rather than bacterial proteins (3), but many of these neutrophil proteins will be phagosomal. Neutrophils stimulated with a phorbol ester displayed protein carbonylation (4) and oxidation of protein thiols (5) in whole cell extracts, but this was an artificial model in which oxidant generation was not restricted to intracellular phagosomes.

The neutrophil proteins most susceptible to oxidative modification have not been identified. Carbonyl groups can be generated on proteins through metal-catalyzed oxidation of arginine, proline, and lysine residues, or by direct reaction with oxidants such as hypochlorous acid and chloramines (6, 7). Protein carbonyls can also result from covalent attachment of electrophilic aldehydes produced during lipid peroxidation, *e.g.* 4-hydroxynonenal (HNE),[3] to cysteine, lysine, and histidine residues (8). The susceptibility of individual residues to modification is influenced by steric features and the effect of the local protein environment on nucleophilicity.

In this study, we quantified protein carbonylation in the cytosol isolated from phagocytic neutrophils and used proteomic techniques to identify those proteins most susceptible to modification. Carbonylation of neutrophil proteins was dependent on NOX2 and myeloperoxidase activity, and inhibitor studies and mass spectrometry analysis revealed a contribution for the products of lipid peroxidation. Cys-2 of S100A9 was shown to be particularly susceptible to modification by HNE in an isolated system. Such post-translational modifications might serve as a biomarker of neutrophil activation during infection or inflammation, and they are also likely to have significant func-

* This work was supported by the Health Research Council of New Zealand, and Ph. D. scholarships from the University of Otago to R. W. and N. M.
[1] Both authors contributed equally to this work.
[2] To whom correspondence should be addressed: Dept. of Pathology, University of Otago, P. O. Box 4345, Christchurch 8140, New Zealand. Tel.: 64-3-378-6225; E-mail: mark.hampton@otago.ac.nz.

[3] The abbreviations used are: HNE, 4-hydroxynonenal; Hsp70, heat shock 70-kDa protein 1; DPI, diphenylene iodonium; IAM, iodoacetamide; NEM, *N*-ethylmaleimide; LC/ESI-MS, liquid chromatography-electrospray mass ionization-mass spectrometry; CTRL, control.

tional implications for the activity of post-phagocytic neutrophils.

EXPERIMENTAL PROCEDURES

Materials—Hypochlorous acid was purchased as commercial chlorine bleach from Household and Body Care (Auckland, New Zealand) and prepared daily at the appropriate concentration using an ϵ_{292} of 350 M^{-1} cm^{-1} at pH 12. Sodium azide was obtained from Fisons Scientific Apparatus (Loughborough, Leicestershire, UK), HNE was from Calbiochem, sodium acetate and formic acid were from Merck (Darmstadt, Germany), ammonium acetate was from J. T. Baker (Phillipsburg, NJ), Diff-Quick was from Dade Behring AG (Dudingen, Switzerland), and Complete™ protease inhibitor cocktail tablets were from Roche Diagnostics (Mannheim, Germany). Regenerable streptavidin-coated magnetic beads were a gift from Anders Holmberg (Dynal Biotech Asa, Oslo, Norway). Bio-Rad DC protein assay, acrylamide/bis solution, ReadyStrip™ 17-cm pH 3–10 immobilized pH gradient strips, and Bio-Lyte® 3/10 ampholytes were from Bio-Rad Laboratories. SYPRO Ruby Protein stain was from Molecular Probes™ supplied by Invitrogen (Auckland, New Zealand). Q Sepharose Fast Flow anion exchanger and SP Sepharose Fast Flow cation exchanger were from GE Healthcare (Buckinghamshire, UK). Amicon Ultra-15® 3K centrifugal filters were from Millipore (Bedford, MA). Sequencing grade modified trypsin was from Promega supplied by In Vitro Technologies (Auckland, New Zealand). The N-terminal S100A9 tryptic peptide, *N*-acetyl-Thr-Cys-Lys, was custom synthesized by GenScript (Piscataway, NJ). All other chemicals were from Sigma-Aldrich.

Staphylococcus aureus—(ATCC 27127, New Zealand Communicable Disease Centre, Porirua) was cultured overnight in trypticase soy broth, harvested and resuspended in Hanks' balanced salt solution (10 mM phosphate buffer, pH 7.4, containing 140 mM NaCl, 0.5 mM $MgCl_2$, 1 mM $CaCl_2$, and 1 mg/ml glucose). Bacterial density was measured at 550 nm relative to a standard curve based on colony-forming units. Bacteria were opsonized with 10% autologous human serum at 37 °C immediately before addition to neutrophils.

Human neutrophils were isolated from heparinized peripheral blood of healthy adult donors under sterile conditions by Ficoll/Hypaque centrifugation, dextran sedimentation, and hypotonic lysis (9). Human neutrophils (10^7/ml) were incubated at 37 °C in RPMI 1640 medium with 10% autologous serum for 10 min at 37 °C in 5% CO_2 for up to 30 min with occasional mixing with opsonized *S. aureus* at ratios of 2, 10, 20, or 50 bacteria per neutrophil.

At selected times, non-phagocytosed bacteria were removed by differential centrifugation at 100 × *g* (10), and the cell pellets were resuspended between 1–2 × 10^7 cells/ml in extract buffer (50 mM NaCl, 1 mM EDTA, 1 mM EGTA, in 40 mM HEPES buffer, pH 7.4, containing protease inhibitor cocktail). The neutrophils were then lysed by nitrogen decompression at 375 p.s.i. for 20 min on ice using a Parr cell disruption vessel 4635 with 1831 nitrogen-filling connection (Parr Instrument Company, Moline, IL). The cell membrane, nuclear, and phagosomal fractions were pelleted by centrifugation at 500 × *g* for 10 min at 4 °C followed by removal of neutrophil granules by centrifugation at 16,100 × *g* for 20 min at 4 °C. The remaining supernatant was the neutrophil cytosol.

Protein concentrations of whole cell neutrophil lysates, 500 × *g* and 16,100 × *g* fractions, and cytosol were calculated using the Bio-Rad DC protein assay kit. Protein carbonyls and myeloperoxidase activity were measured by standard ELISA and 3,3′,5,5′-tetramethylbenzidine oxidation assays as described previously (11, 12).

GSH-HNE adducts were prepared by incubating GSH and HNE at a 4:1 ratio in deionized water for 30 min. The adducts were diluted into a 1:1 methanol/deionized H_2O solution containing 1% (v/v) acetic acid, injected onto a Phenomenex Luna 5-μm C18 column, and measured by LC/MS using a Thermo Finnigan LCQ Deca XP Plus ion trap mass spectrometer coupled to a Thermo Finnigan Surveyor HPLC system (Thermo Finnigan). The HNE-GSH conjugate was eluted with 100% 20 mM ammonium acetate, pH 7, from 0 to 15 min at a flow rate of 200 μl/min. The molecular ion (*m*/*z* 464) was fragmented using 27% collision energy and gave one major fragment ion (*m*/*z* 308). After removal of extracellular bacteria, neutrophils were lysed by resuspending them in 80% (v/v) chilled ethanol followed by sonication. Debris was removed by centrifugation at 16,100 × *g*, and the supernatant was taken to dryness under a vacuum.

Capture of Carbonylated Neutrophil Cytosolic Proteins with Biotin Hydrazide—The isolated cytosols from unstimulated and phagocytic neutrophils were TCA-precipitated, resuspended at 2 mg/ml in 50 mM sodium phosphate buffer, pH 7, containing 5 mM biotin hydrazide, and incubated for 2 h at room temperature. An equal volume of 30 mM sodium cyanoborohydride was added for 5 min followed by TCA precipitation, washed with a 1:1 ethanol/ethyl acetate solution diluted 1:4 with PBS, and resuspended in bead binding buffer (10 mM Tris-HCl, pH 7.5, 1 mM EDTA, 2 M NaCl, 0.1% v/v Tween 20) at 2 mg/ml and added to streptavidin magnetic beads (5 mg/ml) for 15 min at room temperature with intermittent mixing. A magnet was used to collect the beads and washed three times with 10 mM Tris-HCl, pH 7.5, 1 mM EDTA. Magnetic beads were then resuspended in 20 μl of deionized H_2O, heated in a water bath to 70 °C, and held for 30 s. Samples were allowed to cool to room temperature, and the beads were collected using a magnet to leave biotinylated carbonyl proteins in the supernatant.

Immunoblot and Two-dimensional SDS-PAGE Analysis of Neutrophil Cytosolic Proteins—Neutrophil cytosolic extracts or supernatants containing biotinylated carbonyl proteins were resolved by SDS-PAGE and transferred onto PVDF membranes for Western blotting. Blots were probed with rabbit anti-HNE-Michael adduct antibody (1:2000) (Calbiochem), monoclonal mouse MRP14 (1:5000) (Abcam supplied by Sapphire Bioscience Pty. Ltd., Redfern, Australia), or streptavidin-conjugated FITC.

Pooled biotinylated cytosolic carbonyl proteins were separated by two-dimensional SDS-PAGE, using the methodology and equipment described previously (13). Gels were stained with SYPRO Ruby, and the fluorescence was detected by a Bio-Rad Molecular Imager® FX at 488 nm. Protein spots were excised and underwent tryptic digest, reversed-phase zip tip-

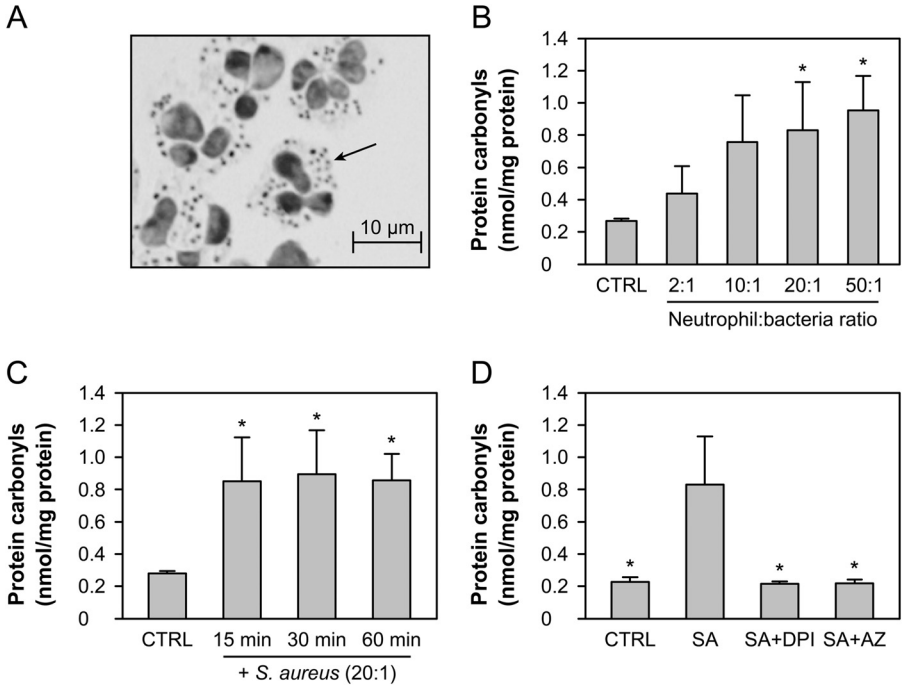

FIGURE 1. **Cytosolic protein carbonyls in phagocytic neutrophils.** *A*, representative photograph taken from a cytospin preparation of human neutrophils co-incubated with *S. aureus* at a 20:1 ratio for 30 min. Phagocytosed *S. aureus* are observed within the cytosol of the neutrophil (*arrow* indicates one example). *B*, neutrophils were incubated alone (*CTRL*) or with *S. aureus* at ratios of 2:1, 10:1, 20:1, and 50:1 bacteria:neutrophil for 30 min, and the carbonyl content of the cytosol was measured by ELISA following nitrogen cavitation and centrifugation. *C*, cytosolic carbonyl levels in neutrophils co-incubated with *S. aureus* (20:1) for the various time intervals indicated. *D*, ELISA cytosolic carbonyl content of neutrophils co-incubated with *S. aureus* (20:1) (*SA*) or treated with 10 μM DPI (*SA+DPI*) or 1 mM azide (*SA+AZ*) prior to co-incubation with *S. aureus* for 30 min. The means and S.E. of three experiments are plotted. A significant difference ($p < 0.05$) from CTRL (*B* and *C*) or *S. aureus* (*D*) is indicated by *.

ping, and analysis by MALDI-TOF mass spectrometry (Centre for Protein Research, Department of Biochemistry, University of Otago).

Purification and Use of Calprotectin from Human Neutrophils—Calprotectin was purified from the cytosol of human neutrophils obtained by nitrogen cavitation using a previously described method (14) with Coomassie Blue staining of reducing SDS-PAGE gels indicating that the purity of calprotectin was 93% with the major contaminant, S100A12, making up 6%. For mass spectrometry and protein carbonyl experiments, calprotectin (40 μM) was incubated with HNE (0–800 μM) in PBS at 37 °C for 30 min. For tryptic digestion, samples were incubated with a 50:1 substrate:trypsin weight ratio at 37 °C for 16 h. Digestion was stopped by the addition of 0.1% v/v final formic acid. *N*-Acetyl-TCK-IAM and *N*-acetyl-TCK-HNE were prepared by incubating *N*-acetyl-TCK in PBS with an excess of iodoacetamide (IAM) or HNE. The relative abundance of each peptide in tryptic digest experiments was standardized based on the sum peak area of peptides in that run that did not significantly change in abundance over all of the experiments (MSQLER, DLQNFLK, and QLSFEEFIMLMAR).

Calprotectin samples analyzed by MALDI-TOF MS were diluted 1 in 5 with matrix (10 mg/ml α-cyano-4-hydroxycinnamic acid dissolved in 65% (v/v) aqueous acetonitrile containing 0.1% (v/v) trifluoroacetic acid and 10 mM ammonium dihydrogen phosphate), spotted onto a MALDI sample plate (Opti-TOF 384-well plate, AB SCIEX, Framingham, MA), and analyzed on a 4800 MALDI-TOF/TOF (AB SCIEX). All MS spectra were acquired in linear, positive-ion mode with 1200 laser pulses per sample spot. The mass range between 1000 and 25,000 was calibrated on a five-peptide/protein calibration mix, and the mass range between 20,000 and 100,000 m/z was calibrated on the singly (66,000 m/z) and doubly charged (33,000 m/z) bovine serum albumin ions. For tryptic digest experiments, precursor ions of interest of each sample spot were selected for MS/MS collision-induced dissociation analysis. For intact protein experiments, S100A12 was used as an internal standard as it contains no cysteine residues (15).

Calprotectin samples analyzed by LC/ESI-MS were injected onto a Phenomenex Jupiter 4-μm Proteo 90A C18 column (150 × 2.0 mm) or a Thermo Hypercarb column (100 × 2.1 mm). Selected reaction monitoring was set up to monitor the most abundant daughter ion of each product after fragmentation. *N*-Acetyl-TCK-IAM was monitored by fragmenting 450.20 m/z and monitoring the 307.14 m/z fragment ion, and *N*-acetyl-TCK-HNE was monitored by fragmenting 549.30 m/z and monitoring the 393.18 m/z fragment ion. Standard curves were constructed for peak area response against the amount of peptide for *N*-acetyl-TCK-IAM and *N*-acetyl-TCK-HNE. The method was sensitive with a detection limit of 600 fmol for *N*-acetyl-TCK-IAM and 60 fmol for *N*-acetyl-TCK-HNE. Native *N*-acetyl-TCK was undetectable after treatment in independent experiments and, therefore, the assumption was made that all of the *N*-acetyl-TCK was modified in each case. IAM (4 mM final) was added to neutrophil cytosol (20 μg/100 μl), collected from *S. aureus*-stimulated and unstimulated neutrophils, and incubated at room temperature for 30 min.

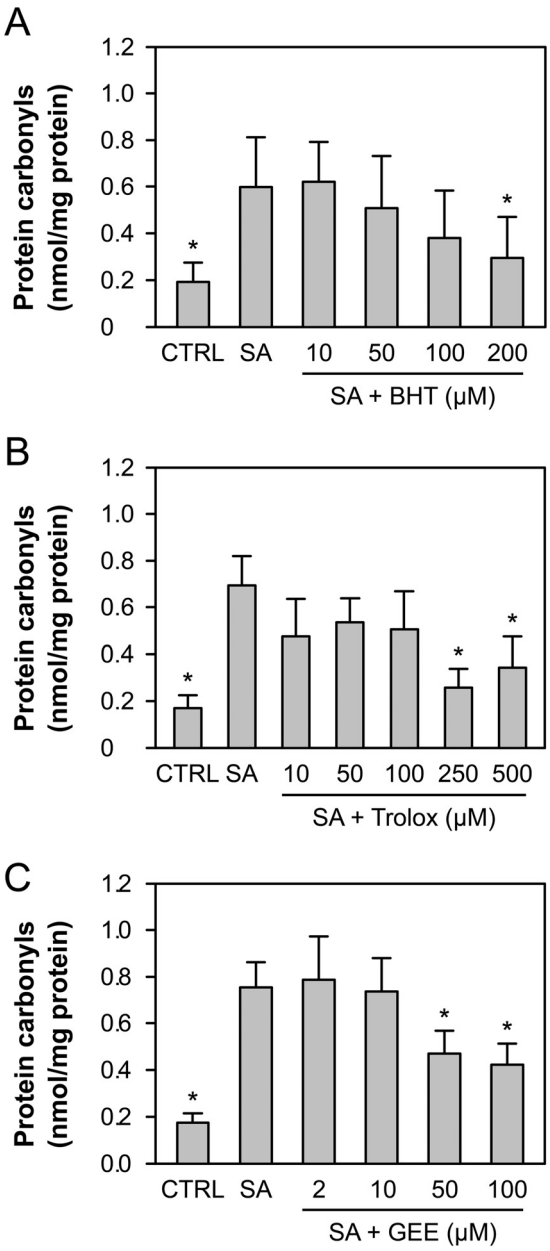

FIGURE 2. **Inhibition of protein carbonyl production in phagocytic neutrophils.** *A–C*, neutrophils were incubated alone (*CTRL*) or treated with varying concentrations of butylated hydroxytoluene (*BHT*) (*A*), Trolox (*B*), or glutathione ethyl ester (*GEE*) (*C*) for 15 min prior to co-incubation with *S. aureus* at a 20:1 ratio (*SA*) for 30 min, and the carbonyl content of the cytosol was measured by ELISA following nitrogen cavitation and centrifugation. The means and S.E. of three experiments are plotted. A significant difference ($p < 0.05$) from the *S. aureus* neutrophils is indicated by *.

Calprotectin Functional Assay—S. aureus was cultured overnight in trypticase soy broth, diluted 1/50 into fresh broth, and cultured for a further 100 min. Exponential phase bacteria were then diluted 1/20 into Chelex-treated broth supplemented with 100 μM $CaCl_2$, 5 μM $FeSO_4$, and 1 mM $MgCl_2$. Bacterial growth was monitored at A_{600} over 6 h in the presence or absence of calprotectin (100 μg/ml), or calprotectin pretreated with HNE.

Statistics—Data are expressed as the means ± S.E. of at least three independent experiments. Graphs and statistics were performed with the SigmaPlot software package (SPSS Science, Chicago, IL) using repeated measures analysis of variance followed by the Holm-Šídák multiple comparison test. Differences were considered significant when the p value was < 0.05.

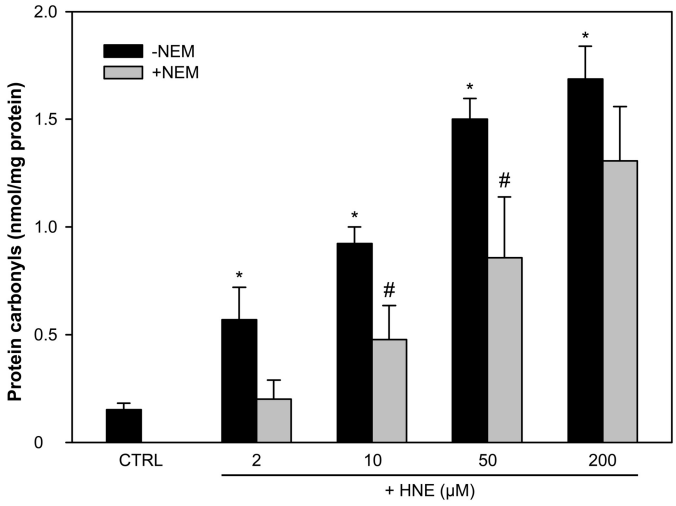

FIGURE 3. **HNE generates protein carbonyls in the cytosol of neutrophils.** The isolated cytosol of DPI-treated phagocytic neutrophils (1 mg/ml) (*CTRL*) was pretreated with or without 10 mM NEM for 15 min before treatment with 2, 10, 50, or 200 μM HNE for 30 min. Protein carbonyl concentrations were measured by ELISA. The means and S.E. of three experiments are plotted. A significant difference ($p < 0.05$) between the control (*CTRL*) and HNE-treated cytosols without NEM is indicated by *. A significant difference ($p < 0.05$) between HNE-treated cytosols with and without NEM is indicated by #.

RESULTS

Protein Carbonyl Formation in Phagocytic Neutrophils—Neutrophils were incubated with opsonized *S. aureus* with occasional mixing at 37 °C. Visual inspection confirmed extensive phagocytosis after 30 min, with all neutrophils containing intracellular bacteria (Fig. 1*A*). Nitrogen cavitation and differential centrifugation were used to separate the cytosol from phagosomes and granules. The cytosol contained 46% (S.D. 8%, $n = 6$) of the total protein of intact neutrophils and only trace amounts of myeloperoxidase activity, confirming successful removal of phagosomes and granules. Protein carbonyls were derivatized with 2,4-dinitrophenylhydrazine and quantified by ELISA. The extent of carbonyl formation in the cytosol of phagocytic neutrophils was dependent on the ratio of bacteria to neutrophils, with carbonylation detectable at a 2:1 ratio and a steady increase as the number of bacteria increased (Fig. 1*B*). The phagocytosis-induced protein carbonyl formation was an early event, with maximum levels observed after only 15 min of co-incubation with *S. aureus*, and not increasing thereafter (Fig. 1*C*). Carbonyl formation was completely blocked in the cytosol of phagocytic neutrophils treated with the NADPH oxidase inhibitor diphenylene iodonium (DPI) and the peroxidase inhibitor sodium azide (Fig. 1*D*). These results indicate that both a functional NADPH oxidase and myeloperoxidase are required to generate protein carbonyls in the cytosol of phagocytic neutrophils.

Two myeloperoxidase-derived oxidants, hypochlorous acid and hypobromous acid, were unable to cause significant carbonylation when added to neutrophils (not shown), and only a very large concentration (100 μM) of dichloramine ($NHCl_2$) was able to significantly increase carbonyl levels (0.643 nmol/mg *versus* 0.187 nmol/mg in the control samples). Therefore, when

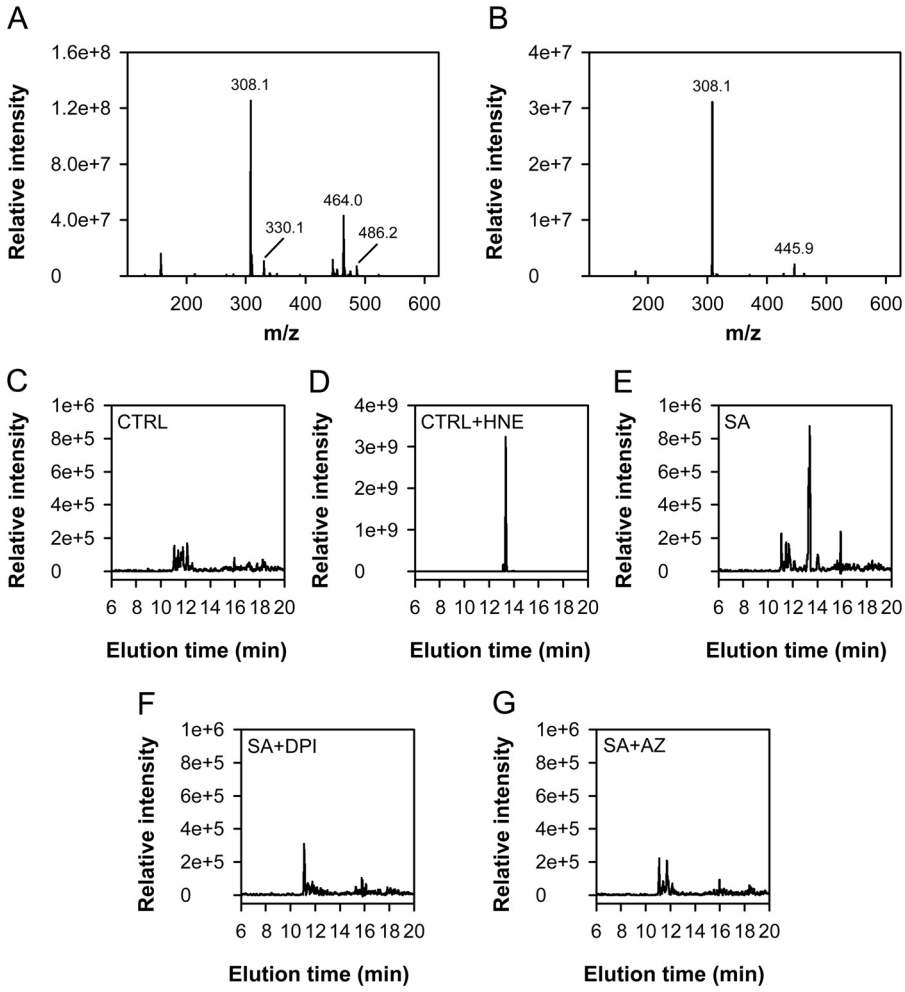

FIGURE 4. **Full and fragmentation mass spectra of the HNE-GSH conjugate.** *A*, full mass spectrum of the HNE and GSH reaction mixture when infused into the mass spectrometer using positive electrospray ionization energy. *B*, fragmentation of the parent ion (*m/z* 464) using 27% collision energy gave one major fragment ion (*m/z* 308). *C–G*, the fragment ion of the HNE-GSH conjugate was monitored by LC/MS in neutrophil lysates 30 min after incubation alone (*CTRL*) (*C*), with 50 μM 4-HNE (*CTRL+HNE*) (*D*), with *S. aureus* (*SA*) at a ratio of 50:1 (*E*), after pretreatment with 10 μM DPI (*SA+DPI*) before co-incubation with *S. aureus* (50:1) (*F*), or after pretreatment with 1 mM azide (*SA+AZ*) for 10 min prior to co-incubation with *S. aureus* (50:1) (*G*). The spectra are representative of two experiments using neutrophils from different donors.

generated in the phagosome, it is most likely that these oxidants react with phagosomal protein rather than carbonylate cytosolic protein. An alternate mechanism of cytosolic protein carbonylation is via reactive aldehydes derived from lipid peroxidation (8). There was a dose-dependent inhibition of cytosolic protein carbonylation when phagocytosis occurred in the presence of the radical scavengers butylated hydroxytoluene and the water-soluble vitamin E analogue Trolox (Fig. 2, *A* and *B*), supporting a contribution by this mechanism. Glutathione ethyl ester is readily taken up by cells and is hydrolyzed by cytosolic esterases to yield GSH. Pretreatment of neutrophils with glutathione ethyl ester was able to partially reduce carbonyl formation in the cytosol of phagocytic neutrophils at concentrations of 50 μM or more, suggesting that thiol-reactive species were responsible for carbonylation (Fig. 2*C*).

To determine whether reactive aldehydes could carbonylate neutrophil proteins, DPI-treated phagocytic neutrophil lysates were incubated with HNE. Extensive carbonylation was detected (Fig. 3). If the cytosolic extracts were first incubated with the thiol alkylator *N*-ethylmaleimide (NEM), there was almost complete inhibition of carbonyl formation at low doses of HNE. This indicates that carbonylation initially occurs on cysteine residues. At higher concentrations of HNE, inhibition by NEM was less effective, suggesting modification of other nucleophilic residues.

To determine whether phagocytosis results in the generation of reactive aldehydes in the neutrophil cytosol, we monitored formation of HNE adducts with reduced GSH. An HNE-GSH standard monitored by positive electrospray ionization mass spectrometry gave a singly protonated ion at *m/z* 464 (Fig. 4*A*) and the major fragment ion *m/z* 308 (Fig. 4*B*). Trace amounts of the fragment ion were detectable in unstimulated neutrophils (Fig. 4*C*), and this increased dramatically in phagocytic neutrophils, indicating significant HNE production upon activation (Fig. 4*E*). Generation of the HNE-GSH adduct was inhibited by DPI and azide (Fig. 4, *F* and *G*).

Identification of Carbonylated Cytosolic Proteins—Carbonylated proteins were derivatized with biotin hydrazide and captured using streptavidin-coated magnetic beads. Significant protein capture was observed only from phagocytic neutrophils

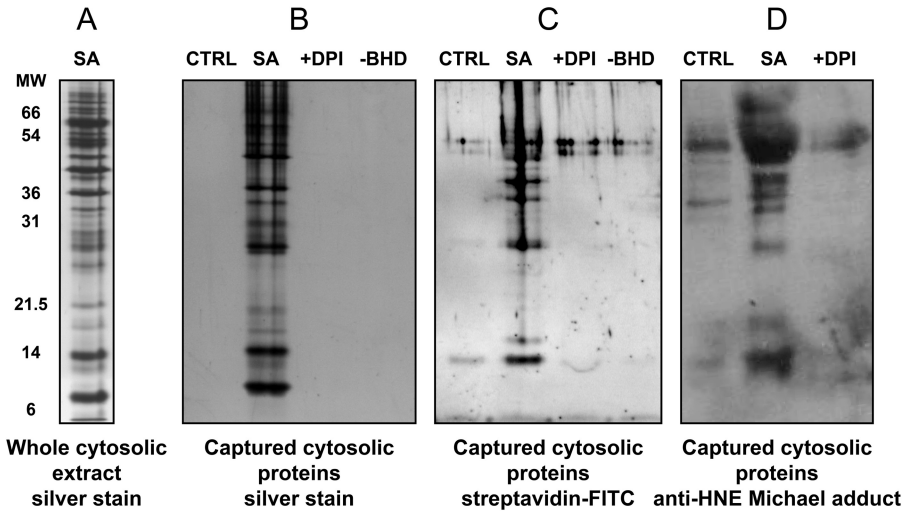

FIGURE 5. **Capture of biotinylated cytosolic carbonyls from phagocytic neutrophils.** Cytosolic extracts of neutrophils treated alone (*CTRL*), treated with *S. aureus* at a 20:1 ratio (*SA*), and treated with DPI prior to co-incubation with *S. aureus* (+*DPI*) were derivatized with biotin hydrazide, and the biotinylated proteins were captured with magnetic streptavidin-coated beads. As a control, neutrophils were treated with *S. aureus* (20:1) but with no biotin hydrazide (−*BHD*). *A*, the whole cytosolic protein extract from neutrophils treated with *S. aureus* (20:1) stained with silver nitrate. *MW*, molecular weight. *B*, biotin hydrazide-derivatized carbonyl proteins captured by magnetic beads were separated by electrophoresis and stained with silver nitrate, *C* and *D*, Western blotted with streptavidin-FITC (*C*) or Western blotted with an HNE-Michael adduct antibody (*D*). The gels are representative of three experiments.

with an active NADPH oxidase, and this was lost in the absence of derivatization with biotin hydrazide (Fig. 5*B*). Comparison with starting material indicated that several of the major proteins were captured, but not all (Fig. 5*A*). Samples were transferred to PVDF membrane and probed with streptavidin-FITC (Fig. 5*C*), thereby revealing the proteins that had been directly biotinylated and not those captured through physical association with a biotinylated protein. The major carbonylated proteins also appeared to contain HNE adducts as assessed with an antibody that recognizes HNE-Michael adducts on proteins (Fig. 5*D*).

The captured proteins were separated by two-dimensional electrophoresis (Fig. 6*A*), excised from the gel, and identified by mass spectrometry (Table 1). The major neutrophil proteins were identified as calprotectin, actin, and heat shock protein 70. Hemoglobin and apolipoprotein A1 were also captured, although they come from erythrocytes and serum present in the assay system. Calprotectin is a major neutrophil cytosolic protein that exists as heterodimer of S100A8 and S100A9 subunits that run at 8 and 14 kDa, respectively, by SDS-PAGE. These subunits correspond to the two major lower bands in Fig. 5, *A* and *B*, of which S100A9 was selectively carbonylated during phagocytosis. As confirmation of calprotectin modification, captured proteins were Western blotted with a monoclonal antibody specific to the S100A9 subunit of calprotectin. Although present in all of the starting extracts, carbonylated S100A9 was captured only in the cytosolic fractions of phagocytic neutrophils, except when DPI was present to inhibit the oxidative burst (Fig. 6*B*).

Characterizing the Reaction of Calprotectin with HNE—Purified calprotectin was treated with various concentrations of HNE, and protein carbonyls were measured by ELISA. Carbonyls were observed at 40 μM HNE and increased progressively with concentrations up to 800 μM (Fig. 7*A*). To determine the relative sensitivities of the subunits to modification, calprotectin was treated with HNE and analyzed by MALDI-TOF MS. S100A9 was most susceptible to modification by HNE with a significant decrease from the control observed with the lowest concentration of HNE (40 μM) (Fig. 7*B*). A truncated S100A9 subunit, missing the first four N-terminal residues (*N*-acetyl-TCKM), only showed a significant decrease from the control when HNE concentrations exceeded 200 μM, and the S100A8 subunit was the least susceptible. A new peak that was 156 molecular mass units higher (one HNE) than the S100A9 subunit was observed following treatment of calprotectin with equimolar HNE (not shown).

To determine which residues were most susceptible to modification, calprotectin was treated with varying concentrations of HNE, digested with trypsin, and analyzed by MALDI-TOF MS and LC/ESI-MS. Five peptides, T1, T3, T4, T13, and T14, had a loss of greater than 20% at calprotectin:HNE molar ratios of up to 1:20, whereas T2, T7, and T12 were unmodified (Fig. 7*C*). All modified peptides contained a cysteine, a histidine, or a lysine residue. Tryptic peptide T1 (*N*-acetyl-TCK), underwent the greatest loss at an equimolar calprotectin:HNE ratio. An HNE adduct was identified on *N*-acetyl-TCK by MS/MS analysis of the parent ion $[M+H]+$ with an m/z value of 549.18 yielding the loss of water and the characteristic loss of HNE (Fig. 7*D*). This adduct must be a HNE-cysteine Michael adduct as modification of the lysine residue would result in a missed cleavage and a merged product with peptide T2. HNE adducts were also identified on six histidine residues (Fig. 7*E*). These results confirm that S100A9 is the calprotectin subunit most susceptible to modification by HNE, and this susceptibility is due to the presence of a reactive cysteine residue near the N-terminal. *N*-Acetyl-TCK-HNE adducts were undetectable by LC/ESI-MS selective reaction monitoring in the cytosols prepared from phagocytic neutrophils.

Calprotectin has been shown to inhibit bacterial growth at inflammatory sites through the chelation of manganese and

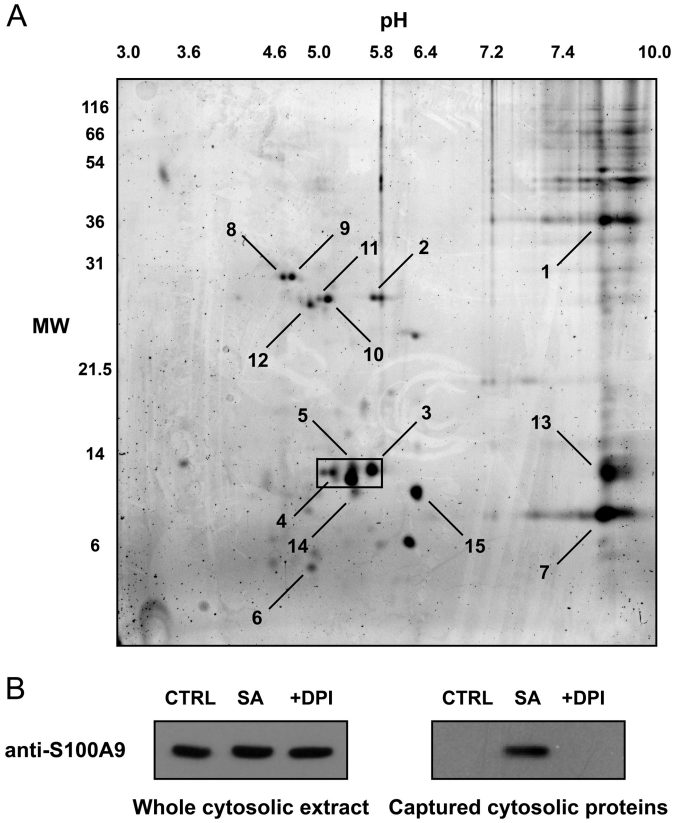

FIGURE 6. **Identification of cytosolic biotin hydrazide-derivatized carbonyl proteins in phagocytic neutrophils by two-dimensional gel electrophoresis and MS.** Cytosolic extracts of neutrophils treated with *S. aureus* at a ratio of 20:1 were derivatized with biotin hydrazide, and the biotinylated proteins were captured with magnetic streptavidin-coated beads. *A*, biotin hydrazide-derivatized carbonyl proteins captured from the beads were separated by two-dimensional electrophoresis with 12% SDS-PAGE in the second dimension. Gels were then stained for total protein with SYPRO Ruby. The gel is representative of seven experiments, and the *boxed region* highlights the 14-kDa proteins that were predominantly captured over the seven experiments. *MW*, molecular weight. *B*, the whole cytosolic extract before bead capture (*left panel*) and the biotinylated proteins captured with magnetic streptavidin-coated beads (*right panel*) were separated by electrophoresis and Western blotted with a specific MRP-14 antibody. The blots are representative of three experiments. *SA*, *S. aureus* (20:1).

zinc (39). Mutation of Cys-2 of S100A9 was shown to inhibit the bacteriostatic properties of calprotectin (39), and the metal binding sites involve several histidine residues. We first confirmed that native calprotectin could inhibit the growth of *S. aureus* (Fig. 8*A*) and that pretreatment of the calprotectin with HNE did indeed block this activity (Fig. 8*B*).

DISCUSSION

We have demonstrated a rapid and substantial increase in protein carbonyls within the neutrophil cytosol following phagocytosis, and inhibitor studies indicated that carbonylation is dependent on the oxidative burst and myeloperoxidase activity. Inhibition of lipid peroxidation was able to block carbonyl formation. Myeloperoxidase-dependent lipid peroxidation has previously been reported (16, 17) and could result from low molecular weight substrates such as tyrosine or urate being oxidized to radicals by compound I or compound II of myeloperoxidase in the phagosome, and then abstracting hydrogen from lipids in the phagosomal membrane to produce radicals.

HNE is a product of arachidonic acid peroxidation (18), and immunocytochemical methods have shown conjugate formation with phagosomal proteins (19). We showed by mass spectrometry that HNE-GSH adducts were produced in phagocytic neutrophils and that HNE-protein adducts could be observed by Western blotting. HNE is freely diffusible and reacts with cellular nucleophiles, particularly sulfhydryl groups of proteins forming thioether adducts via Michael addition.

Derivatization with biotin hydrazide and streptavidin capture was used to identify carbonylated cytosolic proteins. Three major neutrophil proteins were identified: calprotectin, Hsp70, and actin, with the methodology biasing capture of abundant proteins. The spots identified as Hsp70 ran at 28 kDa, less than half of its predicted size. A previous study has shown that oxidatively modified Hsp70, including modification with HNE, was cleaved into a similar sized fragment by calpain in neuronal lysosomes (20). Purified actin has been shown to be susceptible to carbonylation by HNE, particularly Cys-374 (21, 22). This residue is located in a flexible loop region, and although Cys-

TABLE 1

Details of the cytosolic proteins captured by magnetic beads and identified by MALDI-TOF MS

The numbered spots were excised and identified by tryptic digest, MALDI-TOF MS, and matching of the peptide fingerprints with the SwissProt database. Columns marked 2D show the molecular mass (MM) and pI data estimated from the position of the spot in the two-dimensional gel. The molecular mass and pI predicted from the protein sequence data are shown in columns marked Pred. Coverage indicates the percentage of the identified protein covered by the matched peptide masses. Peptide match indicates the number of measured peptide masses that matched the identified protein. The Total ion score column indicates the probability that the observed match between the measured peptide and the database sequence is a random event. For a significant identification ($p < 0.05$), at least one peptide must have an individual ion score ≥44. The total ion score confidence interval (C.I.) is shown and percentages ≥95 are considered statistically significant protein identifications.

Proteins identified	Spot	MM (2D)	pI (2D)	MM (Pred.)	pI (Pred.)	Coverage	Peptide match	Total ion score	C.I.
		kDa		*kDa*		*%*			*%*
Actin-3 subunit 2	1	39.3	8.8	42.6	5.5	4	1	44	96
Calprotectin S100A9 subunit	2	27.7	5.7	13.2	5.7	41	6	386	100
Calprotectin S100A9 subunit	3	13.6	5.7	13.2	5.7	12	2	45	99
Calprotectin S100A9 subunit	4	13.3	5.1	13.2	5.7	53	7	356	100
Calprotectin S100A9 subunit	5	13	5.4	13.2	5.7	28	4	222	100
Calprotectin S100A9 subunit	6	5.9	4.9	13.2	5.7	17	2	98	100
Calprotectin S100A8 subunit	7	9.3	8.8	10.8	6.5	13	2	61	100
Heat shock 70 kDa protein 1	8	29.7	4.6	70.1	5.3	4	1	96	100
Heat shock 70-kDa protein 1	9	29.7	4.7	70.1	5.3	6	3	159	100
Apolipoprotein A1 precursor	10	27.5	5.1	28	5.3	32	11	601	100
Apolipoprotein A1 precursor	11	27.5	4.9	28	5.3	32	10	324	100
Apolipoprotein A1 precursor	12	27	4.9	30.8	5.5	28	11	528	100
Hemoglobin β-subunit	13	13.2	8.8	16	8	22	2	102	100
Streptavidin precursor	14	11.2	5.4	16.5	6.1	26	3	253	100
Streptavidin precursor	15	11.2	6.2	16.5	6.1	10	1	71	100

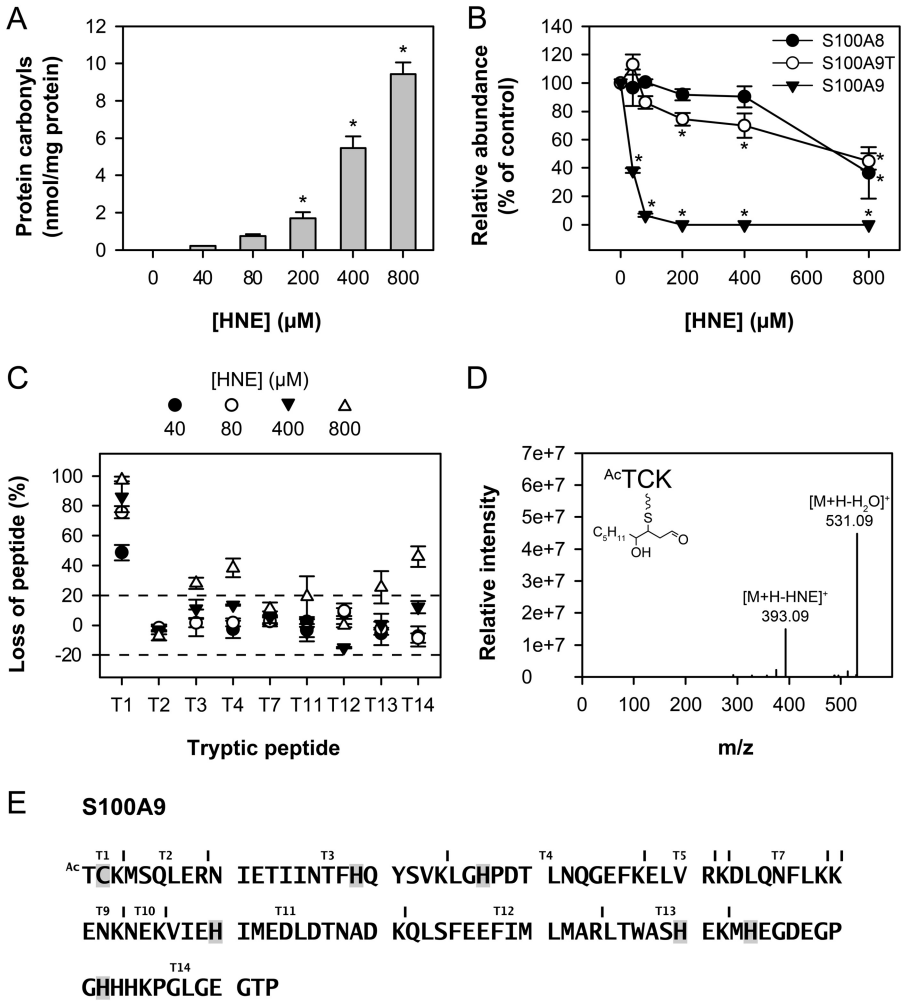

FIGURE 7. **Modification of calprotectin by HNE.** Calprotectin (40 μM) was treated with various concentrations of HNE (0–800 μM). *A*, protein carbonyl measurement of HNE-treated calprotectin. The protein carbonyls formed were derivatized with 2,4-dinitrophenylhydrazine and detected by ELISA. Values represent the means ± S.E. of three separate experiments. A significant difference with the control (0 μM HNE) is indicated by *. *B*, loss of calprotectin subunits induced by HNE treatment. Samples were analyzed using MALDI-TOF MS. The peak height was determined for each subunit, and the relative loss of each subunit was calculated as compared with the control sample for each HNE concentration using S100A12 as an internal standard as it contains no cysteine residues. *S100A9T* = truncated S100A9. Values represent the means ± S.E. of three experiments. A significant difference ($p < 0.05$, one-way analysis of variance, Dunnett's test) with the control (0 μM HNE) is indicated by *. *C*, loss of calprotectin tryptic peptides induced by HNE. Treated protein samples were digested with trypsin overnight and subsequently analyzed using MALDI-TOF MS (or LC/ESI-MS for detection of peptide T1). The peak height response (or product ion peak area response for LC/ESI-MS samples) was determined for each peptide, and the relative loss of each peptide was calculated as compared with the control sample for each HNE concentration. Values represent the means ± S.E. of three separate experiments. Tryptic peptides T1, T3, T4, T13, and T14 were characterized by loss greater than the threshold level (set as 20%). Peptides are labeled as in *E*. *D* and *E*, HNE-modified S100A9 amino acids. Treated protein samples were digested with trypsin overnight and subsequently analyzed by LC/ESI-MS. The *m/z* values of singly and multi-charged state ions corresponding to S100A9 peptides with residues modified by HNE (cysteine, histidine, or lysine) were predicted and matched to LC/ESI-MS fragmentation data (data not shown). The fragmentation pattern of the *N*-acetyl-TCK-HNE peptide is shown in *D*. The MS/MS spectrum was acquired from the ion of *m/z* 549.18 (+1 ion) eluting at 26.94 min. *Ac* = acetylation. Residues determined to be modified by HNE are *highlighted* in *E*.

374-HNE adducts did not alter actin function, saturation of the cysteine led to adduct formation on histidine residues that formed structural distortions of the protein affecting actin polymerization.

Multiple protein spots were observed at the predicted molecular weight of calprotectin. Three isoforms for S100A9 are reported in the literature, and they were demonstrated to have pI values in the ranges we observed (23, 24). The S100A8 and S100A9 subunits of calprotectin are both highly abundant, and each subunit contains one cysteine residue, but only S100A9 was carbonylated. Experiments with recombinant calprotectin showed that S100A9 was significantly more susceptible to modification by HNE than its truncated counterpart or S100A8, and Cys-2 was identified as the primary target. The lower susceptibility of the truncated S100A9 to HNE is consistent with the absence of the reactive cysteine residue. An LC/ESI-MS assay was developed for the detection and quantification of the *N*-acetyl-TCK-HNE adduct of calprotectin, but no adducts were detected in cytosols from phagocytic neutrophils. However, numerous reactive aldehyde species are generated by lipid peroxidation, some of which may be more reactive than HNE, so it may be difficult to detect significant amounts of one particular adduct.

The abundance of calprotectin within the neutrophil cytosol will contribute to its likelihood of carbonylation, but its translocation to the phagosomal membrane may be an important factor. HNE is a major peroxidation product of arachidonic acid, and calprotectin has been shown to bind in a calcium-de-

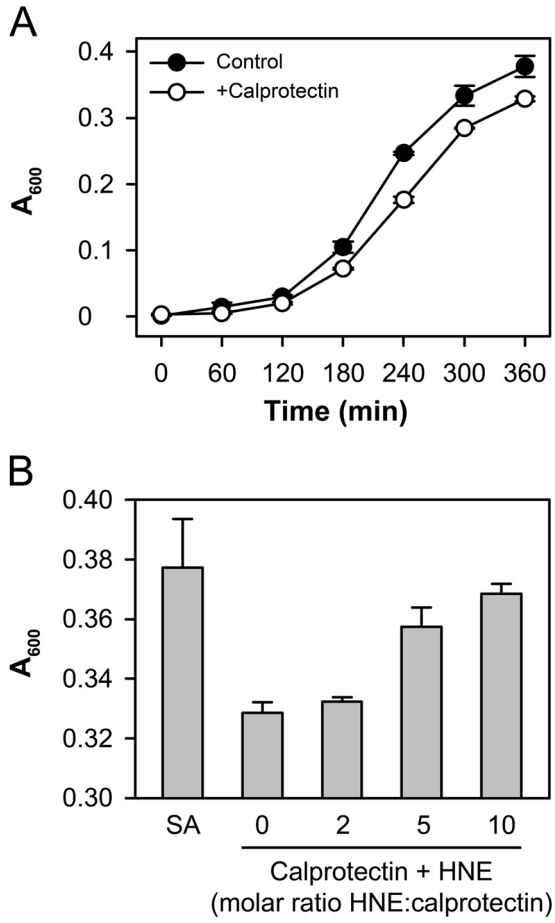

FIGURE 8. **HNE treatment inhibits the bacteriostatic properties of calprotectin.** *A*, the growth of *S. aureus* was monitored at A_{600} over 6 h in Chelex-treated trypticase soy broth in the presence or absence of 100 μg/ml calprotectin. *B*, calprotectin was pretreated with HNE at the indicated molar ratios and then added to the bacteria as in *A*. Bacterial growth at 6 h is shown. A representative experiment is shown due to the variation in the growth rate of bacteria between experiments.

pendent manner to arachidonic acid (25, 26). Elevation of intracellular calcium upon cell activation with zymosan leads to loss of calprotectin and arachidonic acid in the cytosol and an increase in the membrane-associated fraction (24, 27). Calprotectin heterodimers act as a scaffold protein and co-migrate with the NADPH oxidase cytosolic components $p67^{phox}$ and Rac2 (28), promoting NADPH oxidase activation through delivery of arachidonic acid to the NADPH oxidase complex (29, 30). Indeed, the carbonylation of calprotectin reported here may be underestimated if some was still associated with the membranes and removed during the cytosol isolation.

Calprotectin is reported to have chemoattractant and antimicrobial activity (31–33). We showed that HNE modification of calprotectin inhibited the bacteriostatic properties of the protein. This occurred at molar ratios of HNE that modified histidine residues in calprotectin, and is consistent with impairment of metal binding. The N-terminal sequence of S100A9 containing Cys-2 is not essential for calprotectin heterodimer formation, but *S*-glutathionylation of S100A9, which occurs following stimulation of neutrophils with phorbol 12-myristate 13-acetate, decreases binding of the protein to endothelial cells and limits capacity to form heterocomplexes with S100A8 (34). Reversible glutathionylation may, however, protect against carbonylation. It is also interesting to note that S100A9 exists in a full-length and truncated form (missing the first four N-terminal residues (*N*-acetyl-TCKM)) that will be resistant to modification. The truncated form constitutes up to one-quarter of the total neutrophil S100A9 (34).

There are functional implications for the post-translational modification of other neutrophil proteins following activation. The neutrophil was originally considered to be a "kamikaze" cell, quickly destroying itself once activated. However, it is now apparent that neutrophils can live for several hours after activation, and they contribute to regulation of inflammation by releasing cytokines and other inflammatory mediators (35). NOX2 and myeloperoxidase play central roles in post-phagocytic events such as the activation of death pathways and the release of neutrophil extracellular traps (36). The mechanisms of regulation are poorly characterized, but they may involve lipid peroxidation-dependent modification of cytosolic proteins.

Calprotectin is excreted extracellularly from stimulated neutrophils, and levels are increased in inflammatory diseases (37). Calprotectin levels are currently monitored as a marker of neutrophil presence during inflammation, particularly as a fecal marker in inflammatory bowel disease (38). This work has shown that calprotectin is susceptible to oxidative modification in phagocytic neutrophils. Identification of specific adducts or oxidation products may provide novel biomarkers of neutrophil activation that better correlate with inflammatory disease.

Acknowledgments—We thank Dr Torsten Kleffmann and Diana Carne for performing the MALDI-TOF MS analyses.

REFERENCES

1. Babior, B. M. (1999) NADPH oxidase: an update. *Blood* **93,** 1464–1476
2. Hampton, M. B., Kettle, A. J., and Winterbourn, C. C. (1998) Inside the neutrophil phagosome: oxidants, myeloperoxidase, and bacterial killing. *Blood* **92,** 3007–3017
3. Chapman, A. L., Hampton, M. B., Senthilmohan, R., Winterbourn, C. C., and Kettle, A. J. (2002) Chlorination of bacterial and neutrophil proteins during phagocytosis and killing of *Staphylococcus aureus*. *J. Biol. Chem.* **277,** 9757–9762
4. Oliver, C. N. (1987) Inactivation of enzymes and oxidative modification of proteins by stimulated neutrophils. *Arch. Biochem. Biophys.* **253,** 62–72
5. Chai, Y. C., Ashraf, S. S., Rokutan, K., Johnston, R. B., Jr., and Thomas, J. A. (1994) *S*-Thiolation of individual human neutrophil proteins including actin by stimulation of the respiratory burst: evidence against a role for glutathione disulfide. *Arch. Biochem. Biophys.* **310,** 273–281
6. Requena, J. R., Chao, C. C., Levine, R. L., and Stadtman, E. R. (2001) Glutamic and aminoadipic semialdehydes are the main carbonyl products of metal-catalyzed oxidation of proteins. *Proc. Natl. Acad. Sci. U.S.A.* **98,** 69–74
7. Vissers, M. C., and Winterbourn, C. C. (1991) Oxidative damage to fibronectin. I. The effects of the neutrophil myeloperoxidase system and HOCl. *Arch. Biochem. Biophys.* **285,** 53–59
8. Uchida, K., and Stadtman, E. R. (1993) Covalent attachment of 4-hydroxynonenal to glyceraldehyde-3-phosphate dehydrogenase: a possible involvement of intra- and intermolecular cross-linking reaction. *J. Biol. Chem.* **268,** 6388–6393
9. Böyum, A. (1968) Separation of leukocytes from blood and bone marrow. Introduction. *Scand. J. Clin. Lab. Invest. Suppl.* **97,** 7
10. Hampton, M. B., Vissers, M. C., and Winterbourn, C. C. (1994) A single

assay for measuring the rates of phagocytosis and bacterial killing by neutrophils. *J. Leukoc. Biol.* **55,** 147–152
11. Buss, H., Chan, T. P., Sluis, K. B., Domigan, N. M., and Winterbourn, C. C. (1997) Protein carbonyl measurement by a sensitive ELISA method. *Free Rad. Biol. Med.* **23,** 361–366
12. Chapman, A. L., Mocatta, T. J., Shiva, S., Seidel, A., Chen, B., Khalilova, I., Paumann-Page, M. E., Jameson, G. N., Winterbourn, C. C., and Kettle, A. J. (2013) Ceruloplasmin is an endogenous inhibitor of myeloperoxidase. *J. Biol. Chem.* **288,** 6465–6477
13. Baty, J. W., Hampton, M. B., and Winterbourn, C. C. (2002) Detection of oxidant sensitive thiol proteins by fluorescence labeling and two-dimensional electrophoresis. *Proteomics* **2,** 1261–1266
14. Yousefi, R., Imani, M., Ardestani, S. K., Saboury, A. A., Gheibi, N., and Ranjbar, B. (2007) Human calprotectin: effect of calcium and zinc on its secondary and tertiary structures, and role of pH in its thermal stability. *Acta Biochim. Biophys. Sin. (Shanghai)* **39,** 795–802
15. Ilg, E. C., Troxler, H., Bürgisser, D. M., Kuster, T., Markert, M., Guignard, F., Hunziker, P., Birchler, N., and Heizmann, C. W. (1996) Amino acid sequence determination of human S100A12 (P6, calgranulin C, CGRP, CAAF1) by tandem mass spectrometry. *Biochem. Biophys. Res. Commun.* **225,** 146–150
16. Zhang, R., Brennan, M. L., Shen, Z., MacPherson, J. C., Schmitt, D., Molenda, C. E., and Hazen, S. L. (2002) Myeloperoxidase functions as a major enzymatic catalyst for initiation of lipid peroxidation at sites of inflammation. *J. Biol. Chem.* **277,** 46116–46122
17. Heinecke, J. W. (2002) Tyrosyl radical production by myeloperoxidase: a phagocyte pathway for lipid peroxidation and dityrosine cross-linking of proteins. *Toxicology* **177,** 11–22
18. Esterbauer, H., Schaur, R. J., and Zollner, H. (1991) Chemistry and biochemistry of 4-hydroxynonenal, malonaldehyde and related aldehydes. *Free Radic. Biol. Med.* **11,** 81–128
19. Quinn, M. T., Linner, J. G., Siemsen, D., Dratz, E. A., Buescher, E. S., and Jesaitis, A. J. (1995) Immunocytochemical detection of lipid peroxidation in phagosomes of human neutrophils: correlation with expression of flavocytochrome b. *J. Leukoc. Biol.* **57,** 415–421
20. Sahara, S., and Yamashima, T. (2010) Calpain-mediated Hsp70.1 cleavage in hippocampal CA1 neuronal death. *Biochem. Biophys. Res. Commun.* **393,** 806–811
21. Dalle-Donne, I., Carini, M., Vistoli, G., Gamberoni, L., Giustarini, D., Colombo, R., Maffei Facino, R., Rossi, R., Milzani, A., and Aldini, G. (2007) Actin Cys374 as a nucleophilic target of α,β-unsaturated aldehydes. *Free Radic. Biol. Med.* **42,** 583–598
22. Aldini, G., Dalle-Donne, I., Vistoli, G., Maffei Facino, R., and Carini, M. (2005) Covalent modification of actin by 4-hydroxy-*trans*-2-nonenal (HNE): LC-ESI-MS/MS evidence for Cys374 Michael adduction. *J. Mass Spectrom.* **40,** 946–954
23. Guignard, F., Mauel, J., and Markert, M. (1996) Phosphorylation of myeloid-related proteins MRP-14 and MRP-8 during human neutrophil activation. *Eur. J. Biochem.* **241,** 265–271
24. Roulin, K., Hagens, G., Hotz, R., Saurat, J. H., Veerkamp, J. H., and Siegenthaler, G. (1999) The fatty acid-binding heterocomplex FA-p34 formed by S100A8 and S100A9 is the major fatty acid carrier in neutrophils and translocates from the cytosol to the membrane upon stimulation. *Exp. Cell Res.* **247,** 410–421
25. Kerkhoff, C., Klempt, M., Kaever, V., and Sorg, C. (1999) The two calcium-binding proteins, S100A8 and S100A9, are involved in the metabolism of arachidonic acid in human neutrophils. *J. Biol. Chem.* **274,** 32672–32679
26. Klempt, M., Melkonyan, H., Nacken, W., Wiesmann, D., Holtkemper, U., and Sorg, C. (1997) The heterodimer of the Ca^{2+}-binding proteins MRP8 and MRP14 binds to arachidonic acid. *FEBS Lett.* **408,** 81–84
27. Lemarchand, P., Vaglio, M., Mauël, J., and Markert, M. (1992) Translocation of a small cytosolic calcium-binding protein (MRP-8) to plasma membrane correlates with human neutrophil activation. *J. Biol. Chem.* **267,** 19379–19382
28. Doussiere, J., Bouzidi, F., and Vignais, P. V. (2002) The S100A8/A9 protein as a partner for the cytosolic factors of NADPH oxidase activation in neutrophils. *Eur. J. Biochem.* **269,** 3246–3255
29. Kerkhoff, C., Nacken, W., Benedyk, M., Dagher, M. C., Sopalla, C., and Doussiere, J. (2005) The arachidonic acid-binding protein S100A8/A9 promotes NADPH oxidase activation by interaction with $p67^{phox}$ and Rac-2. *FASEB J.* **19,** 467–469
30. Bouzidi, F., and Doussiere, J. (2004) Binding of arachidonic acid to myeloid-related proteins (S100A8/A9) enhances phagocytic NADPH oxidase activation. *Biochem. Biophys. Res. Commun.* **325,** 1060–1065
31. Harrison, C. A., Raftery, M. J., Walsh, J., Alewood, P., Iismaa, S. E., Thliveris, S., and Geczy, C. L. (1999) Oxidation regulates the inflammatory properties of the murine S100 protein S100A8. *J. Biol. Chem.* **274,** 8561–8569
32. Lusitani, D., Malawista, S. E., and Montgomery, R. R. (2003) Calprotectin, an abundant cytosolic protein from human polymorphonuclear leukocytes, inhibits the growth of *Borrelia burgdorferi*. *Infect. Immun.* **71,** 4711–4716
33. Sohnle, P. G., Hunter, M. J., Hahn, B., and Chazin, W. J. (2000) Zinc-reversible antimicrobial activity of recombinant calprotectin (migration inhibitory factor-related proteins 8 and 14). *J. Infect. Dis.* **182,** 1272–1275
34. Lim, S. Y., Raftery, M. J., Goyette, J., and Geczy, C. L. (2010) *S*-Glutathionylation regulates inflammatory activities of S100A9. *J. Biol. Chem.* **285,** 14377–14388
35. Mantovani, A., Cassatella, M. A., Costantini, C., and Jaillon, S. (2011) Neutrophils in the activation and regulation of innate and adaptive immunity. *Nat. Rev. Immunol.* **11,** 519–531
36. Parker, H., Dragunow, M., Hampton, M. B., Kettle, A. J., and Winterbourn, C. C. (2012) Requirements for NADPH oxidase and myeloperoxidase in neutrophil extracellular trap formation differ depending on the stimulus. *J. Leukoc. Biol.* **92,** 841–849
37. Poullis, A., Foster, R., Mendall, M. A., and Fagerhol, M. K. (2003) Emerging role of calprotectin in gastroenterology. *J. Gastroenterol. Hepatol.* **18,** 756–762
38. Røseth, A. G., Schmidt, P. N., and Fagerhol, M. K. (1999) Correlation between faecal excretion of indium-111-labelled granulocytes and calprotectin, a granulocyte marker protein, in patients with inflammatory bowel disease. *Scand. J. Gastroenterol.* **34,** 50–54
39. Corbin, B. D., Seeley, E. H., Raab, A., Feldmann, J., Miller, M. R., Torres, V. J., Anderson, K. L., Dattilo, B. M., Dunman, P. M., Gerads, R., Caprioli, R. M., Nacken, W., Chazin, W. J., and Skaar, E. P. (2008) Metal chelation and inhibition of bacterial growth in tissue abscesses. *Science* **319,** 962–965